JOURNAL OF Materials CHEMISTRY

Functional homo- and heterometallic alkoxides as precursors for sol–gel routes to transparent $ZnGa_2O_4$ coatings

Stephane Daniele, Dmitry Tcheboukov and Liliane G. Hubert Pfalzgraf*

Université Claude Bernard Lyon 1, IRC, 2 avenue A. Einstein, 69626 Villeurbanne cedex, France. E-mail: hubert@catalyse.univ-lyon1.fr

Received 5th April 2002, Accepted 22nd May 2002
First published as an Advance Article on the web 28th June 2002

New homo- and heterometallic $[M(OR)_3]_m$ and $[ZnM_2(OR)_8]_m$ species (M = Al, Ga; R = C_2H_4OMe, $C_2H_4NMe_2$) have been prepared and characterised by elemental analysis, electrospray mass spectrometry, FT-IR and multinuclear NMR. Hydrolyses of the heterometallic compounds were investigated and the particle sizes were determined. The thermal behaviour of the hydrolysed products was studied by TGA/DTA and the nature of the phases was analysed by powder X-ray diffraction. Various sol–gel processing parameters were studied in order to stabilise nanosized colloidal suspensions for access to thin films by spin coating. $[ZnGa_2(OC_2H_4OMe)_8]_2$ was the best candidate for sol–gel processing, allowing crystalline $ZnGa_2O_4$ solids to be obtained at 300 °C. Films, obtained on glass and MgO substrates, were transparent (>95%) and characterised by UV-visible and X-ray photoelectron spectroscopies, tapping mode AFM, SEM, EDX and X-ray diffraction.

Introduction

Modern technologies require new materials, such as, for instance, multimetallic oxides having specific and controlled properties. Their preparation from metal–organic precursors by "chimie douce" generally has the advantages over solid state routes of lower temperatures of crystallisation and better compositional uniformity of the final material. However, these processes require oxide precursors having appropriate physical and chemical properties. Metal alkoxides have attracted much attention due to their solubility in a wide variety of organic solvents and their ability to form heterometallic species.[1] Transparent and conductive oxide (TCO) films are of particular importance due to their applications in optics and electronics. Tin oxide doped with In_2O_3 has been the subject of many investigations.[2] Zinc-based materials such as ZnM_2O_4 (M = Al,[3a] M = Ga[3b]) have gained attention more recently for such applications. Zinc gallate was reported as a prospective low voltage phosphor material,[3b] and films were obtained by CVD from zinc and gallium acetylacetonates or from $Zn[GaMe_2(\mu\text{-}O^iPr)_2]_2$.[4] Access to Zn–In oxides was essentially investigated by physical methods.[5] Solution routes, namely metal organic decomposition (MOD) or sol–gel techniques for access to gallium oxide-based materials, such as oxidation catalysts[6a] or TCO oxides, *e.g.* $ZnGa_2O_4$, have used gallium salts (with zinc salts for the latter) as raw materials.[6b] Gallium and indium alkoxides $M(OR)_3$ (M = Ga, In; R = Me, Et, ^{n}Pr, ^{i}Pr, ^{n}Bu, ^{t}Bu)[7] were first reported by Mehrotra *et al.* Other homoleptic gallium alkoxides based on bulky groups were prepared more recently and used for CVD of Ga_2O_3 films.[8] A number of gallium alkylalkoxides are also known, but their hydrolytic susceptibility is inappropriate for sol–gel applications.[9]

We wish to report here our investigations on homo and heterometallic precursors of $ZnAl_2O_4$ and $ZnGa_2O_4$ based on functional alkoxide ligands, namely methoxyethoxide and dimethylaminoethoxide. These were characterised by elemental analysis, FT-IR, NMR (^{1}H, ^{27}Al) and mass spectrometric data. $ZnGa_2(OC_2H_4OMe)_8$ was used for access to transparent $ZnGa_2O_4$ films by spin coating.

Experimental

All manipulations were performed under dry argon using Schlenk tube techniques. Solvents and alcohols were purified by standard methods and stored over molecular sieves. $Al(OC_2H_4OMe)_3$,[10] $ZnAl_2(O^iPr)_8$,[11] $Zn(OC_2H_4X)_2$ (X = OMe, NMe_2),[12] $Ga[N(SiMe_3)_2]_3$[13] and $Ga(NEt_2)_3$[14] were prepared as reported in the literature. FT-IR spectra were recorded from Nujol mulls on a Perkin-Elmer Paragon 500 FT-IR spectrometer. UV-visible spectra were recorded on a Unicam UV2-100 spectrometer. NMR spectra were obtained on a Bruker AM-300 spectrometer, the ^{27}Al NMR spectra were recorded at 78.20 MHz, $Al(NO_3)_3$ was used as an external reference. Analytical data were obtained from the Centre de Microanalyses du CNRS. TGA/DTA data were collected on a Setaram 92 system under argon with a thermal ramp of 5 °C min^{-1}. Powder X-ray diffraction data were obtained with a Siemens D 5000 diffractometer using Cu-Kα radiation. Particle sizes were measured in solution with a Coulter N4 Plus submicron particle sizer. Cells were filled with solvent and 6–10 drops of the hydrolyzed solutions were added to achieve a scattering intensity of 5×10^4–1×10^6 counts s^{-1} at 90°. XPS experiments were performed with a VG Scientific Escalab 200R spectrometer using monochromated Al-Kα radiation as the excitation source. FAM and SEM images were collected on Digital Instruments Nanoscope III and Hitachi S800 spectrometers, respectively.

The glass or MgO (Crystec Gmbh) substrates were cleaned with acetone and dried at 100 °C. 0.1 ml of solution (0.1 M, h = 4) was dropped rapidly on the substrate, spinning at a speed of 3000 rpm for 1 min. The film was then dried at 100 °C for 30 min and the whole procedure repeated six times. The films were annealed at 600 °C (heating rate 10 °C min^{-1}) for either 1 or 10 h in air.

Syntheses

$[Al(OC_2H_4OMe)_3]_2$ (1). 2-Methoxyethanol (15 ml) was added to $Al(O^iPr)_3$ (2.7 g, 13.67 mmol) in toluene (10 ml). After refluxing for 4 h, distillation *in vacuo* gave a colorless oil (**1**) (3.44 g, 99%). Anal.: calcd for $C_9H_{21}O_6Al$: C 42.8, H 8.3,

Al 10.7; found C 42.3, H 8.6, Al 11.4%. IR (cm^{-1}): 1365 s, 1331 w, 1289 w, 1246 m, 1199 vs, 1163 m, 1154 m, 1124 vs, 1093 vs, 1072 vs, 1023 s, 964 m, 940 s, 912 s, 839 s, 679 s; 567 m, 538 w, 465 w, 451 w ν(Al–OR). ^{1}H NMR (δ, $CDCl_3$): 4.28 (dt, ^3J = 4.3, ^2J = 9.8 Hz, 3H, OCH_2), 4.17 (t, ^3J = 4.9 Hz, 6H, OCH_2), 4.01 (dt, ^3J = 4.3, ^2J = 9.8 Hz, 3H, OCH_2), 3.66 (dt, ^3J = 4.3, ^2J = 7.6 Hz, 3H, OCH_2), 3.58 (t, ^3J = 4.9 Hz, 6H, OCH_2), 3.45 (dt, ^3J = 4.3, ^2J = 7.6 Hz, 3H, OCH_2), 3.32 (s, 9H, OMe), 3.29(s, 9H, OMe). ^{27}Al NMR (δ, toluene-d_8): 7.42 ($\Delta\nu_{1/2}$ = 175 Hz). MS (m/z^+, %): $Al_2(OR)_5$ (429, 7); $Al_2(OR)_4(OC_2H_4)$ (398, 4); $Al_2(OR)_4(OMe)$ (385, 100); $Al_2(OR)_4$ (354, 19); $Al_2(OR)_3(OMe)$ (341, 41); $Al_2(OR)_3(OMe)$ (310, 11); $Al_2(OR)(OMe)_3$ (297, 8); $Al(OR)_2(OMe)$ (209, 10); $Al(OR)_2$ (177, 80); Al(OR)(OMe) (133, 43); $Al(OR)_2$ (103, 18); $AlO(OC_2H_4)$ (89, 6).

$[Ga(OC_2H_4OMe)_3]_2$ (2). A solution of 1.45 ml (18.39 mmol) of 2-methoxyethanol in 20 ml of toluene was added to $Ga[N(SiMe_3)_2]_3$ (3.1 g, 5.6 mmol) in toluene (15 ml). After stirring for 15 h, refluxing for 6 h and distillation to eliminate excess of 2-methoxyethanol, the solvent was removed *in vacuo*, yielding **2** as a colourless oil (1.44 g, 87%). The same product was obtained by reacting $Ga(NEt_2)_3$ (1.05 g, 3.68 mmol) in 10 ml THF with 1 ml of methoxyethanol (13 mmol) for 12 h (1.0 g, 92%) Anal.: calcd for $C_9H_{21}O_6Ga$: C 36.6, H 7.1, Ga 23.7; found C 37.1, H 7.2, Ga 23.1%. IR (cm^{-1}): 1364 s, 1330 w, 1290 w, 1245 m, 1198 s, 1127 vs, 1091 vs, 1070 vs, 1025 s, 986 w, 964 m, 921 s, 904 s, 841 s, 798 w; 694 w; 620 s, 511 s ν(Ga–OR) ^{1}H NMR (δ, $CDCl_3$): 4.11 (dt, ^3J = 4.9, ^2J = 11.3 Hz, 3H, OCH_2), 4.03–3.86 (overlapping m, 3H, OCH_2), 3.95 (t, ^3J = 5.8 Hz, 6H, OCH_2), 3.65–3.45 (overlapping m, 6H, OCH_2), 3.46 (t, ^3J = 5.8 Hz, 6H, OCH_2); 3.42 (s, 9H, OMe), 3.36 (s, 9H, OMe).

$[Ga(OC_2H_4NMe_2)_3]_2$ (3). 2-Dimethylaminoethanol (7 ml) in toluene was added to 0.62 g (1.1 mmol) of $Ga[N(SiMe_3)_2]_3$ in toluene. After stirring at room temperature for 15 h and refluxing for 12 h, the volatiles were removed, giving a light-yellow oil which crystallised after 1–2 days. Recrystallisation in hexane at −25 °C gave crystals of **3** (0.2 g, 54%). **3** was soluble in all standard organic solvents. The same product (0.1 g, 45%) was obtained by reacting $Ga(NEt_2)_3$ (0.15 g, 0.7 mmol) in petroleum ether with 0.2 ml (2.1 mmol) of dimethylaminoethanol. Anal.: calcd for $C_{12}H_{30}O_3N_3Ga$: C 43.1, H 8.9, N 12.5, Ga 20.9; found C 42.9, H 8.6, N 12.9, Ga 21.2%. IR (cm^{-1}): 1405 w, 1351 m, 1276 m, 1258 s, 1197 s, 1184 m, 1106 s, 1097 vs, 1074 s, 1029 s, 948 vs, 916 w, 886 s, 842 w, 786 m, 621 w; 605 s, 563 s, 528 s ν(Ga–N, Ga–O). ^{1}H NMR (δ, $CDCl_3$): 3.85 (br, 12H, OCH_2), 2.55 (br, 12H, NCH_2), 2.32 (s, NMe_2, 36H).

$[ZnAl_2(OC_2H_4X)_8]_m$ {X = OMe, *m* = 3 (4); X = NMe_2, *m* = 2 (5)}. *Method A.* $Al(OC_2H_4OMe)_3$ (1.06 g, 4.2 mmol) in toluene (15 ml) was added to a suspension of $Zn(OC_2H_4OMe)_2$ (0.45 g, 2.1 mmol) in the same solvent. Dissolution occurred in 30 min. The volatiles were removed after 12 h, giving **4** as a colourless viscous oil (1.4 g, 90%).

Method B. **4** was also obtained by alcohol exchange reaction of $ZnAl_2(O^iPr)_8$ (0.92 g, 1.6 mmol) with 2-methoxyethanol (1.02 ml, 13.4 mmol) in toluene (25 ml) and removal of the volatiles by distillation (1 g, 89%). Anal.: calcd for $C_{24}H_{56}O_{16}Al_2Zn$: C 40.0, H 7.8, Al 7.5, Zn 9.1; found C 40.5, H 7.9, Al 7.7, Zn 9.3%. IR (cm^{-1}): 1394 w, 1331 m, 1289 w, 1255 sh, 1244 m, 1198 s, 1160 sh, 1124 vs, 1095 vs, 1082 vs, 1024 s, 985 w, 965 m, 932 s, 915 sh, 841 s, 803 w; 676 s, 637 s, 597 m, 566 m, 508 s, 469 s ν(M–OR). ^{1}H NMR (δ, $CDCl_3$): 3.74 (t, J = 5.6 Hz, 48H, OCH_2), 3.36 (t, J = 5.6 Hz, 48H, OCH_2), 3.32, 3.30, 3.23 (s, [3 : 2 : 1], 72H, OMe). ^{27}Al NMR (δ, toluene-d_8): 8.23 ($\Delta\nu_{1/2}$ = 210 Hz), 37.4 ($\Delta\nu_{1/2}$ = 2800 Hz), 66 ($\Delta\nu_{1/2}$ = 3100 Hz) [1 : 1 : 1].

Procedure B applied to 0.21 g (0.35 mmol) of $ZnAl_2(O^iPr)_8$ and 0.3 ml (3 mmol) of 2-dimethylaminoethanol in 30 ml of toluene gave $[ZnAl_2(OC_2H_4NMe_2)_8]_2$ (**5**) as a colorless oil (0.27 g, 93%). Anal.: calcd for $C_{32}H_{80}O_8N_8Al_2Zn$: C 46.6, H 9.7, N 13.6, Al 6.55, Zn 7.9; found C 46.9, H 9.9, N 13.3, Al 6.7, Zn 8.1%. IR (cm^{-1}): 1405 w, 1383 m, 1365 w, 1325 w, 1262 s, 1186 m, 1120 vs, 1100 vs, 1074 s, 1054 s, 1042 s, 1024 s, 952 s, 902 m, 817 m, 805 s, 786 s, 710 s, 673 s, 645 w, 559 w, 511 w, 479 m, 461 m. ^{1}H NMR (δ, C_6D_6): 4.03 (t, J = 6.2 Hz, 32H, OCH_2), 2.45 (t, J = 6.2 Hz, 32H, NCH_2), 2.28 (s, 96H, NMe_2). ^{27}Al NMR (δ, toluene-d_8): 9.12 ($\Delta\nu_{1/2}$ = 375 Hz), 34.0 ($\Delta\nu_{1/2}$ = 138 Hz), 71.7 ($\Delta\nu_{1/2}$ = 513 Hz) ($\approx$10 : 1 : 2).

$[ZnGa_2(OC_2H_4OMe)_8]_2$ (6). $Ga(OC_2H_4OMe)_3$ (**2**) (0.633 g, 2.1 mmol) in toluene (15 ml) was added to a suspension of $Zn(OC_2H_4OMe)_2$ (0.22 g, 1.05 mmol) in the same solvent. Dissolution occurred in 30 min. After stirring for 12 h, the volatiles were removed, giving a light-yellow viscous oil (**6**) (1.4 g, 89%). Anal.: calcd for $C_{24}H_{56}O_{16}Ga_2Zn$: C 35.8, H 7.0, Ga, 17.3, Zn, 8.1; found C 36.1, H 7.3, Ga, 17.5, Zn, 8.2%. IR (cm^{-1}): 1394 w, 1330 w, 1287 w, 1244 s, 1198 vs, 1127 vs, 1076 vs, 1024 vs, 986 w, 963 m, 906 s, 840 s, 734 m; 631 m, 515 w. ^{1}H NMR (δ, $CDCl_3$): 3.91 (t, ^3J = 5.3 Hz, 32H, OCH_2), 3.49 (t, ^3J = 5.3 Hz, 32H, OCH_2), 3.43 (s, 48H, OMe).

Results and discussion

1 Homometallic precursors

Aluminium 2-methoxyethoxide was prepared by alcohol exchange reaction applied to the isopropoxide. The gallium alkoxides $[Ga(OR)_3]_m$ (R = C_2H_4OMe, $C_2H_4NMe_2$) were prepared by alcoholysis of amides according to eqn. 1. The sterically encumbered gallium trimethylsilylamide[15] was less reactive than its indium counterpart and its alcoholysis required refluxing for a few hours; alcoholysis of the more reactive trisdiethylamide was thus used as an alternative.

$$\underset{R=Et,\ SiMe_3}{M(NR_2)_3} + 3\ ROH \xrightarrow[20\ ^\circ C]{toluene} \underset{\substack{R=C_2H_4OMe,\ M=Al(1,\ 99\%),\ Ga(2,\ 87\%)\\ R=C_2H_4NMe_2,\ M=Ga(3,\ 54\%)}}{1/m[M(OR)_3]_m} + 3\ HNR_2 \qquad (1)$$

Gallium 2-methoxyethoxide is a viscous liquid, whereas the 2-dimethylaminoethoxide is a crystalline solid. All compounds were soluble and/or miscible in THF, diethyl ether, toluene and the parent alcohol. The 2-dimethylaminoethoxide was also readily soluble in aliphatic hydrocarbons. The new compounds could not be distilled or sublimed in the range 100–200 °C/10^{-3} Torr. They were characterised by elemental analyses, and FT-IR and NMR spectroscopy. IR spectra showed no absorption bands due to ν(OH) vibrations and, thus, confirmed the absence of species solvated by the parent alcohol.

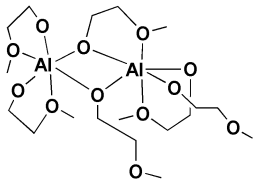

A

The ^{1}H NMR spectra of the aluminium and gallium 2-dimethoxyethoxides (**1** and **2**) showed comparable patterns. The ^{1}H NMR spectra of **1** displayed two sets of resonances (integration ratio 1 : 1) for the three types of protons $MOCH_2$, CH_2O and OMe. The $MOCH_2$ hydrogens appeared as diastereotopic methylene protons, giving rise to two AB quintets at 4.28 and 4.01 ppm (^3J = 4.3, ^2J = 9.8 Hz), indicating the proximity of a prochiral atom. Dilution (0.15–0.02 M) had no effect on the integration ratio, suggesting the presence of a

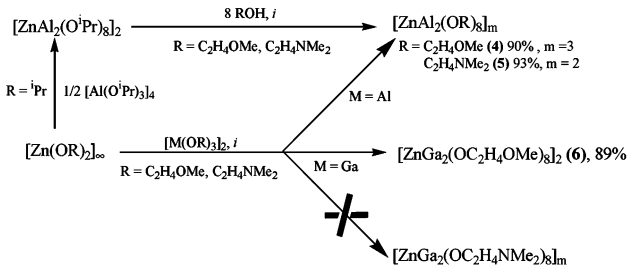

Scheme 1 Synthesis of compounds **4–6**. *Reagents and conditions*: (*i*) toluene, 20 °C, 2 h.

single fluxional molecular species in solution. The ^{27}Al NMR spectrum of **1** at 293 K displayed only a sharp signal at 7.42 ppm with a line width of 175 Hz, indicating the presence of six-coordinated aluminium centres.[16] The mass spectral data provide evidence for the existance of dimeric species. The presence of signals due to the OMe groups in a 1 : 1 ratio may be attributed to ligands coordinated in η^2- and η^1-coordination modes, with dangling ether functions for the latter, as for structure **A**. Such a structure is also supported by the X-ray structure determination of the $[In_2(\mu,\eta^1\text{-OR})(\mu,\eta^2\text{-OR})(\eta^2\text{-OR})_3(\eta^1\text{-OR})]$ ($R = C_2H_4NMe_2$) dimer.[17]

The ^{1}H NMR spectra of the gallium dimethylaminoethoxide (**3**) at room temperature showed only one set of resonances. These uninformative spectra might be attributable to dynamic processes on the NMR time scale, faster than for **1** and **2**, or to quadrupolar relaxation phenomena, but no low temperature investigation could be achieved.

2 Heterometallic precursors

Heterometallic Zn–Al and Zn–Ga compounds were prepared by mixing $[Zn(OR)_2]_\infty$ and $[M(OR)_3]_2$ (M = Al, Ga; R = C_2H_4OMe, $C_2H_4NMe_2$) in toluene at room temperature in a 1 : 2 stoichiometry (Scheme 1). Dissolution of the polymeric zinc methoxyethoxide or dimethylaminoalkoxide occurred in each case. The formation of the heterometallic species **4–6** was confirmed by FT-IR and NMR data different from those of the starting alkoxides. On mixing $[Zn(OC_2H_4NMe_2)_2]_\infty$ and $[Ga(OC_2H_4NMe_2)_3]_2$, no reaction was observed despite refluxing in toluene for 2 h, and the initial zinc alkoxide was totally recovered by precipitation during concentration of the reaction medium. Elemental analysis confirmed that the Zn : M ratio (M = Al, Ga) of compounds **4–6** was 1 : 2, corresponding to that in the targeted oxides. $[ZnAl_2(OR)_8]_m$ (R = C_2H_4OMe and $C_2H_4NMe_2$) could also be obtained by alcohol exchange reaction under azeotropic distillation conditions from the heterometallic $ZnAl_2(O^iPr)_8$ species. Compounds **4–6** were viscous oils, miscible with THF, diethyl ether, toluene and the parent alcohol, but not with aliphatic hydrocarbons. Electrospray mass spectrometric data in acetonitrile suggest that **4** is a trimer ($m = 3$) and **5** and **6** are both dimers ($m = 2$).[18] Room temperature ^{1}H NMR spectra of **4–6** displayed only one set of resonance for the OCH_2, CH_2X (X = O, N) and OMe or NMe_2 groups, thus suggesting the existance of fluxional processes. On cooling a solution of $ZnAl_2(OC_2H_4NMe_2)_8$ in $C_6D_5CD_3$ to 188 K, the triplet at 4.03 ppm (–OCH_2–) was split into five signals (4.43, 4.30, 4.08, 3.96 and 3.56 ppm) displaying a 3 : 1 : 2 : 1 : 1 integration ratio. Its ^{27}Al NMR spectrum at 293 K displayed an important sharp signal at 9.12 ppm (in the range of six-coordinated aluminium) and two minor broader signals at 34.0 and 71.7 ppm (in the range of five- and four-coordinated aluminium centres, respectively). Heterometallic alkoxides of MM'_2 stoichiometry can display various frameworks, namely open-shell and *closo* structures.[19] Representative structures of non-oxo alkoxides of MM'_2 stoichiometry with metals in similar oxidation states are those of $MgAl_2(O^sBu)_8$[20] and of $Mg_2Sb_4(OEt)_{10}$.[21] According to the NMR data, the major species present in non polar solutions of **5** could be depicted as structure **B** (or its isomers) with hexacoordinated metals and derived from the original dinuclear $Al_2(OR)_6$ moiety. Opening of one or two of the chelates affording additional dangling nitrogens and η^1-coordination might lead to the five- and four-coordinated aluminium centres, respectively, as observed by ^{27}Al NMR. The Zn–Ga aminoethoxide **6**, which is also observed to be dinuclear by ESMS, presumably has the same framework.

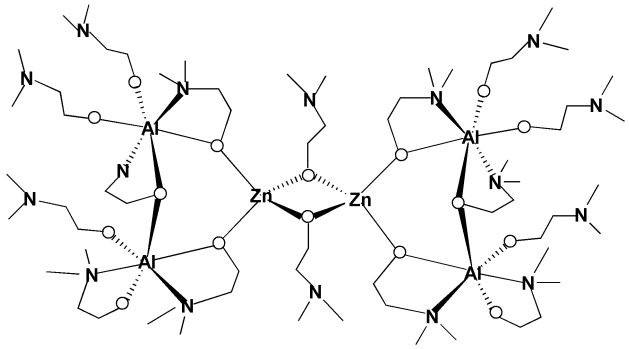

3 Hydrolyses

Hydrolyses of the heterometallic $[ZnM_2(OR)_8]_m$ (**4–6**) compounds were performed at room temperature. A number of factors, namely solvent (THF, ^{i}PrOH, parent alcohol, parent alcohol with acetone as co-solvent), concentration (0.1–1 M) and hydrolysis ratio, $h = [H_2O]/[ZnM_2(OR)_8]$ ($h = 8$, 100), were investigated in order to optimise the crystallisation conditions of the mixed oxides. The resulting amorphous powders were obtained by evaporation to dryness of the reaction mixtures and characterised by FT-IR, TGA/DTA and XRD after thermal treatment. They all present some organic residues (FT-IR evidence), but these can be eliminated below 400 °C, as shown by TGA/DTA data. The TGA/DTA data for **4–6** were similar, with: (i) an endothemic process around 100 °C due to loss of adsorbed solvent or water, (ii) an important exothermic process around 300 °C due to pyrolysis of residual organics and (iii) several small exothermic processes due either to further combustion or crystallisation phenomena. The last processes, observed in the range 520–765 °C and occurring without weight loss, were attributed to crystallisation (Fig. 1). The results are summarised in Table 1.

The solvent and the nature of the alkoxide ligand (R = ^{i}Pr, C_2H_4OMe, $C_2H_4NMe_2$) have little influence on the temperature of crystallisation of ZnM_2O_4, although the hydrolytic behaviour is different. Turbid gels were obtained with solutions (1 M) of $ZnAl_2(O^iPr)_8$ and $ZnAl_2(OC_2H_4NMe_2)_8$. The use of

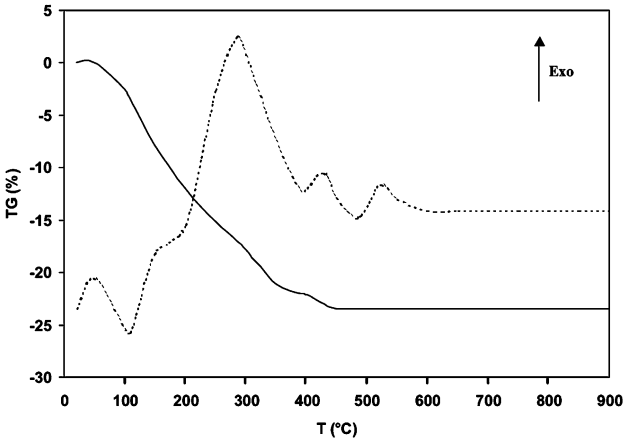

Fig. 1 TGA (—) and DTA (- - -) data of the powder resulting from hydrolysis of **6**.

Table 1 Hydrolyses of $ZnM_2(OR)_8$ (M = Al, Ga; R = ^{i}Pr, C_2H_4OMe, $C_2H_4NMe_2$)

Precursor	Solvent	Conc./mol L^{-1}	h	DTA peak/°C	Oxide phase
$[ZnAl_2(O^iPr)_8]_2$	HO^iPr	0.1	8	623	$ZnAl_2O_4$
	HO^iPr	1	8	641	$ZnAl_2O_4$
	THF	0.2	8	662	$ZnAl_2O_4$
$[ZnAl_2(OC_2H_4OMe)_8]_3$ (**4**)	HOC_2H_4OMe	0.1	8	595	$ZnAl_2O_4$
	HOC_2H_4OMe	1	8	765	$ZnAl_2O_4$
	HOC_2H_4OMe	0.1	100	654	$ZnAl_2O_4$
	HOC_2H_4OMe + acetone (1 : 1)	0.1	8	613	$ZnAl_2O_4$
	HO^iPr	0.1	8	650	$ZnAl_2O_4$
$[ZnAl_2(OC_2H_4NMe_2)_8]_2$ (**5**)	THF	0.1	8	583	$ZnAl_2O_4$
	THF	0.2	8	673	$ZnAl_2O_4$
	HO^iPr	0.1	8	601	$ZnAl_2O_4$
$[ZnGa_2(OC_2H_4OMe)_8]_2$ (**6**)	HOC_2H_4OMe	0.1	8	518	$ZnGa_2O_4$
	HOC_2H_4OMe	1	8	675	$ZnGa_2O_4$
$[Zn(OC_2H_4NMe_2)_2]_\infty$ + 2 $[Ga(OC_2H_4NMe_2)_3]_m$	THF	0.1	8	593	$ZnGa_2O_4$
	THF	0.2	8	682	$ZnGa_2O_4$

acetone as a co-solvent, the latter being known to induce non-hydrolytic condensation, especially with zinc alkoxides,[22] and thus to decrease the temperature of crystallisation, also had no noticeable effect. By contrast, high Zn–M solution concentrations and high hydrolysis ratios led to the highest temperatures of crystallisation. Very short gelation times were observed under such conditions ($\approx$30 s compared to 0.5–1 h in other cases), this could result in matrices being more dense and, thus, to higher combustion temperatures for residual organics (weight losses up to about 800 °C).

The calcinated powders have been characterised by XRD at variable temperatures. They all indicated the formation of the pure spinel phase. Fig. 2 shows the XRD patterns of as-prepared and the heat-treated $ZnGa_2O_4$ powders under different temperatures (JCPDS file no. 86-0413). The onset of crystallisation occurs at 300 °C, this is about 150 °C lower than for $ZnAl_2O_4$ obtained from the hydrolysis of $ZnAl_2(OC_2H_4OMe)_8$. Although the crystallinity of this powder was poor at 450 °C, it should be noted that those resulting from the hydrolysis of Al *sec*-butoxide and $Zn(OAc)_2{\cdot}3H_2O$ were amorphous up to 600 °C.[23] The value of using the heterometallic precursor $[ZnGa_2(OC_2H_4OMe)_8]_2$ *vs.* using a mixture of homometallic precursors $[Zn(OC_2H_4NMe_2)_2]_\infty$ and $[Ga(OC_2H_4NMe_2)_3]_2$, providing no homogeneity at a molecular level, is illustrated by the increase of crystalline quality and the reduction of about 100 °C in the crystallisation temperature of $ZnGa_2O_4$. The broad peaks indicate very small crystallites. The size of the $ZnGa_2O_4$ particles at 300 °C, estimated from the Debye–Scherrer formula, is about 4.8 nm. $ZnAl_2O_4$ and $ZnGa_2O_4$ nanoparticles were sintered at 300, 400, 500, 600, 700, 800 and 900 °C for 10 h under air. Their XRD peaks became sharper with increasing temperature, yielding nanoparticles of about 8 and 20 nm, respectively.

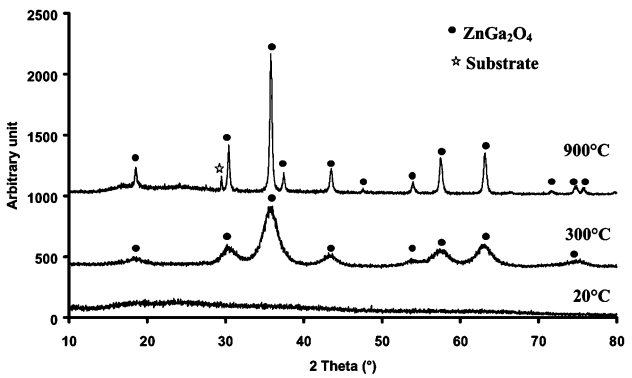

Fig. 2 XRD patterns of as-prepared and heat-treated $ZnGa_2O_4$ powders.

4 Preparation of colloidal suspensions, elaboration of films

Colloidal suspensions or gelous media are usually required for the elaboration of thin films *via* solution routes.[2] The stability of the colloidal media is also of importance for industrial applications, hence, partial hydrolysis and aging phenomena were investigated. Partial hydrolyses were performed by mixing 0.05 M solutions of $[ZnGa_2(OC_2H_4OMe)_8]_2$ in HOC_2H_4OMe with a 2 M solution of water in the same solvent, to achieve h = 1, 2, 4, 5, 6, 8. Hydrolyzed solutions were stored under argon for 1 week at room temperature and evolution of the particle size in solution was recorded by light scattering measurements. The diagram in Fig. 3 collects the various observations and shows the evolution of the particle size as a function of time. Hydrolysis for $h < 4$ gave air-sensitive solutions which were difficult to handle and had poor stability. Hydrolysis for h = 5–6 led to very viscous sols which resulted in blue gels after 2 h. These gels were reversible by shaking, giving sols of large particles (about 1500 nm). For h = 8, precipitates were observed after a few hours (particle sizes larger than 2500 nm). For h = 4, transparent blue sols were obtained after 12 h. They were stable for 2 days and based on particles of about 150–200 nm. They were used to elaborate $ZnGa_2O_4$ films by spin coating at a speed of 3000 rpm. This procedure was followed by drying of the film at 100 °C for 30 min and repeated six times. The films were annealed at 600 °C (10 °C min^{-1}) for 1 or 10 h in air. The use of higher viscosity samples by employing more concentrated solutions (>0.1 M) lead to poor coverage of the substrate.

5 Characterisation of the films

$ZnGa_2O_4$-coated glass and MgO annealed at 600 °C for 1 or 10 h had good mechanical resistance as well as a very good

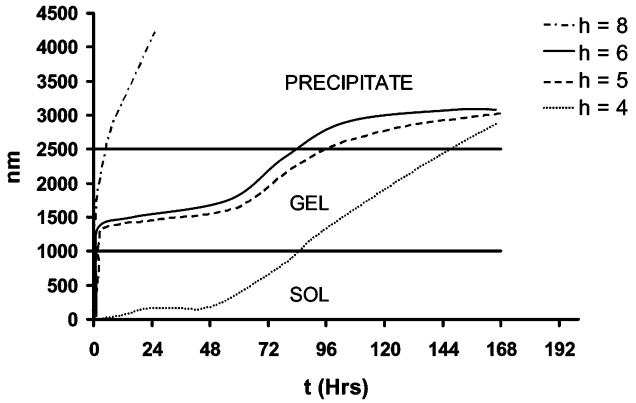

Fig. 3 Particle size evolution as a function of time for partially hydrolysed $[ZnGa_2(OC_2H_4OMe)_8]_2$ (**6**) solutions.

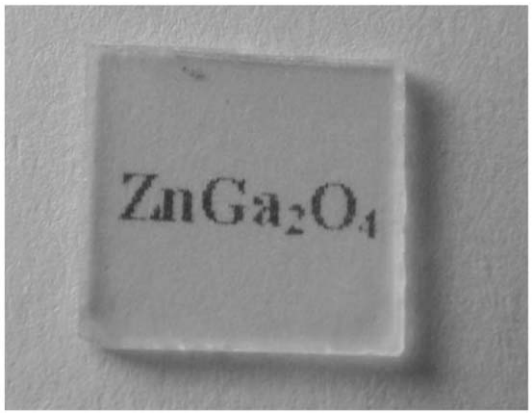

Fig. 4 Picture of $ZnGa_2O_4$ films deposited on MgO annealed at 600 °C.

transparency by UV-visible spectroscopy. A transmittance of 90–95% was observed between 350–900 nm for six deposits (Fig. 4). SEM micrographs of a cross-section showed the stacking with an overall thickness of 1.6 μm for the films (Fig. 5). XRD of the films showed only the spinel $ZnGa_2O_4$ phase and the particle size estimated from the Debye–Scherrer formula was about 13.3 nm, compared to 8.8 nm for the powder [Fig. 6(b)]

XPS spectra recorded from 0 to 1200 eV indicated that the films contained zinc, gallium, oxygen and a significant amount of carbon. In the absence of depth profiling analysis of the film composition, it has not been possible to determined whether this is due to surface contamination or film incorporation. Surprisingly, a Ga/Zn atomic ratio of 4 was observed, which suggests a gallium-rich surface. EDX measurements on the cross-section of the films confirmed this unexpected metal stoichiometry. Furthermore, they showed that the distribution between the metals was inhomogeneous within the film. On the other hand, XPS spectra of powders resulting from hydrolysis of **6** and annealed at 600 °C displayed the expected 1 : 2 Zn : Ga ratio. Tapping force atomic microscopy measurements of the film indicated a rough surface (mean roughness of 25 nm) and magnification showed the presence of hexagonal crystallites at the surface. [Fig. 6(a)]. The overall data suggest that the Zn : Ga stoichiometry of $ZnGa_2O_4$ is disrupted by interaction with the glass substrate. Thus, the result is a multiphasic material, namely crystallites of $ZnGa_2O_4$ in an amorphous matrix of zinc and gallium oxides. It is noteworthy that the films of $ZnGa_2O_4$ obtained by CVD showed a similar deviation

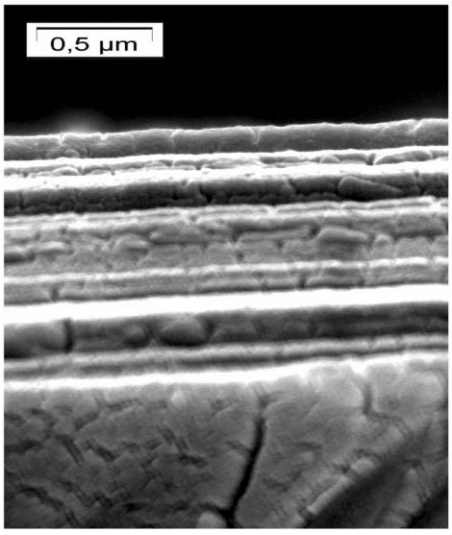

Fig. 5 Cross-sectional SEM picture of a $ZnGa_2O_4$ film deposited on soda glass annealed at 600 °C.

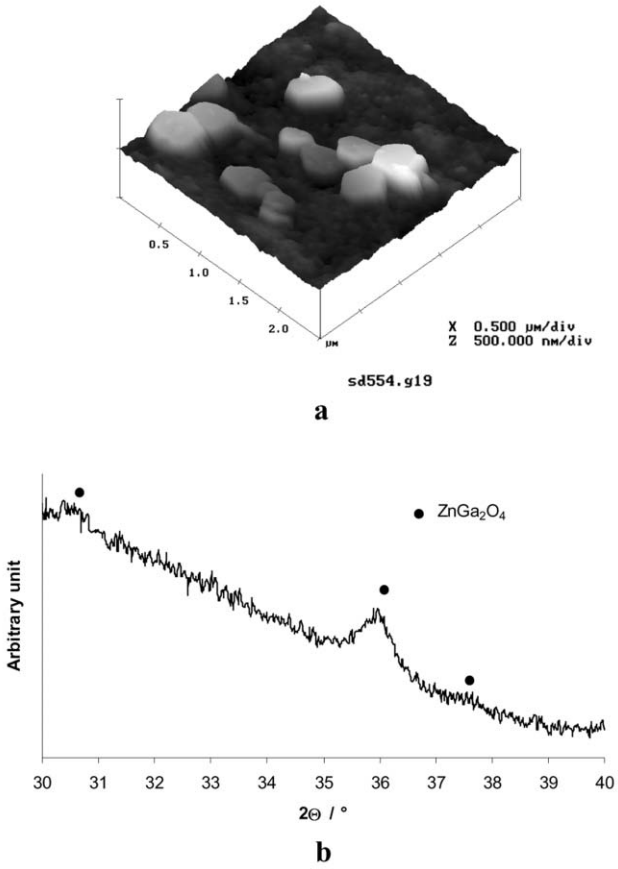

Fig. 6 (a) AFM image and (b) XRD pattern of Zn–Ga films deposited on soda glass annealed at 600 °C.

from the Zn : Ga 1 : 2 stoichiometry by XPS, but this was attributed to the dissociation of the Zn–Ga species and loss of a zinc derivative in the vapour phase.[4] The interaction between glass and the $ZnGa_2O_4$ coating was confirmed by the fact that deposition on an MgO substrate and thermal annealing under similar conditions than for the previous deposits gave XPS data confirming the retention of the Zn : Ga 1 : 2 stoichiometry. XRD of those films showed the spinel $ZnGa_2O_4$ phase and the particle size estimated from the Debye–Scherrer formula was about 17.0 nm [Fig. 7(b)]. Tapping mode atomic force microscopy measurements of the film on MgO showed fine spherical grains without any cracks and a mean roughness of 40 nm [Fig. 7(a)]. Attempts to measure the thickness by SEM was precluded, since no difference in contrast could be evidenced between the substrate and the deposit, thus indicating a dense and uniform film.

Conclusion

New homo and heterometallic $[M(OR)_3]_m$ and $[ZnM_2(OR)_8]_m$ species (M = Al, Ga, R = C_2H_4OMe, $C_2H_4NMe_2$) were prepared and characterised by elemental analysis, electrospray mass spectrometry, FT-IR and multinuclear NMR. Stable colloidal suspensions were obtained by controlled hydrolysis (h = 4) of $[ZnGa_2(OC_2H_4OMe)_8]_2$ in the parent alcohol and were used to elaborate deposits by spin coating. Films, obtained on glass or MgO substrates and annealed at 600 °C for 1 h, were transparent (>95%) and characterised by UV-visible spectroscopy, XPS, AFM, SEM, EDX and XRD. $ZnGa_2O_4$ films on MgO substrates were homogeneous with fine spherical grains and a mean roughness of 40 nm. The homogeneity of the films on glass was, however, lost due to interaction with the substrate, as shown by XPS and AFM

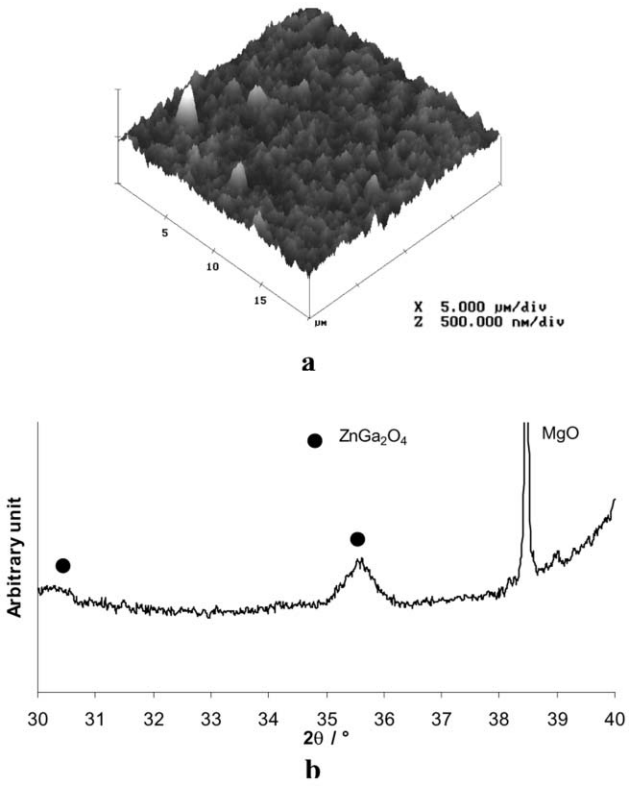

Fig. 7 (a) AFM image and (b) XRD pattern of $ZnGa_2O_4$ films deposited on MgO annealed at 600 °C.

data, resulting in hexagonal crystallites of $ZnGa_2O_4$ in an amorphous matrix of zinc and gallium oxides.

Acknowledgements

D. T. is grateful for a Nato fellowship. We thank G. Wicker, P. Delichere and C. Deranlot for the SEM/EDX, XPS and AFM measurements, respectively.

References

1 L. G. Hubert-Pfalzgraf, *Coord. Chem. Rev.*, 1998, **178–180**, 967.
2 M. Guglielmi, E. Menegazzo, M. Paolizzi, G. Gasparro, D. Ganz, J. Putz, M. A. Aegerter, L. G. Hubert-Pfalzgraf, C. Pascual, A. Duran, H. X. Willems, M. Van Bommel, L. Buttgenbach and L. Costa, *Sol-Gel Sci. Technol.*, 1998, **13**, 679 and refs. therein; T. Kanbara, M. Nagasaka and T. Yamamoto, *Chem. Mater.*, 1990, **2**, 643; N. E. Trofimenko, S. V. Boron, N. P. Masherovo and K. A. Lesnikovich, *Russ. J. Appl. Chem.*, 1995, **68**, 397.
3 (*a*) S. Mathur, M. Veith, M. Haas, H. Shen, N. Lecerf, V. Huch, S. Hufner, R. Haberkorn, H. P. Beck and M. Jilavi, *J. Am. Ceram. Soc.*, 2001, **84**, 1921; (*b*) S. Itoh, H. Toki, Y. Sato, K. Morimoto and T. Kishino, *J. Electrochem. Soc.*, 1991, **138**, 1509; (*c*) H. Takatsuji, T. Hirimori, K. Tsujimoto, S. Tsuji, K. Kuroda and H. Saka, *Mater. Res. Soc. Symp. Proc.*, 1998, **508**, 315.
4 M. A. McCoy, R. W. Robin and W. E. Lee, *Philos. Mag. A*, 1997, **76**, 1187; S. Naghavi, C. Marcel, L. Dupont, A. Rougier, J. B. Leriche and C. Guéry, *J. Mater. Chem.*, 2000, **10**, 2315 and refs. therein.
5 C. G. Kim, W. Koh, S.-J. Ku, E. J. Nah, K. S. Yu and Yu. Kim, *Mater. Res. Soc. Symp. Proc.*, 1999, **510**, 562; G. C. Kim, J. S. Kim, E. S. Oh, J. C. Char, K. Jeong, S. K. Chang, H. L. Park, T. W. Kim and C. D. Kim, *Mater. Res. Bull.*, 2000, **35**, 2409.
6 (*a*) C. Otero Arean, A. L. Bellan, M. P. Mentruit, M. P. Delgado and G. T. Palomino, *Microporous Mesoporous Mater.*, 2000, **40**, 35; (*b*) T. Sei, Y. Normura and T. Tsuchiya, *J. Non-Cryst. Solids*, 1997, **218**, 135; (*c*) M. Hirano, S. Okumura, Y. Hasegawa and M. Inagaki, *Int. J. Inorg. Mater.*, 2001, **3**, 797.
7 A. Mehrotra and R. C. Mehrotra, *Inorg. Chem.*, 1972, **11**, 2170; S. Chatterjee, S. R. Bindal and R. C. Mehrotra, *J. Indian Chem. Soc.*, 1976, **53**, 867; S. R. Bindal, V. K. Mathur and R. C. Mehrotra, *J. Chem. Soc. A*, 1969, 863; R. C. Mehrotra, A. Singh and S. Sogani, *Chem. Rev.*, 1994, **94**, 1643; D. C. Bradley, H. Chudzynska, D. M. Frigo, M. E. Hammond, M. B. Hursthouse and M. A. Mazid, *Polyhedron*, 1990, **9**, 719; J. P. Oliver, R. Kumar and M. Taghliof, *Coord. Chem. Rev.*, 1993, **167**, 15.
8 L. A. Miinea, S. Suh and D. M. Hoffmann, *Inorg. Chem.*, 1999, **38**, 4447; S. Suh and D. Hoffman, *J. Am. Chem. Soc.*, 2000, **122**, 9396.
9 K. H. Thiele, E. Hecht, T. Gelbricht and U. Duemichen, *J. Organomet. Chem.*, 1997, **540**, 89; H. Schumann, M. Frick, B. Hymer and F. Girgsdis F., *J. Organomet. Chem.*, 1996, **512**, 117; W. Cleaver, A. R. Barron, M. Mcgufey and S. G. Bott, *Polyhedron*, 1994, **13**, 2831; H. Schumann, J. Kaufmann, S. Dechert, H. Schmalz and J. Velder, *Tetrahedron Lett.*, 2001, **42**, 5405.
10 A. Alipour, H. Jazayeri and M. Mohammadpour Amini, *J. Coord. Chem.*, 2000, **51**, 319.
11 M. Aggrawal and R. C. Mehrotra, *Synth. React. Inorg. Met.-Org. Chem.*, 1988, 9.
12 S. C. Goel, M. Y. Chiang and W. E. Buhro, *Inorg. Chem.*, 1990, **29**, 4646.
13 H. Burger, J. Cichon, U. Goetze, U. Wannagat and H. J. Wismar, *J. Organomet. Chem.*, 1971, **33**, 1.
14 H. Nöth and P. Konrad, *Z. Naturforsch., B*, 1975, **30**, 681.
15 M. Niemeyer, T. J. Goodwin, S. H. Risbud and P. P. Power, *Chem. Mater.*, 1996, **8**, 2745; M. F. Lappert, A. R. Sanger, P. P. Power and R. C. Srivastava, *Metal and Metalloid Amides*, Ellis Horwood, Chichester, 1980.
16 J. W. Akitt, *Prog. Nucl. Magn. Reson. Spectrosc.*, 1989, **21**, 1.
17 S. Daniele, D. Tcheboukov, L. G. Hubert-Pfalzgraf and S. Lecocq, *Inorg. Chem. Commun.*, 2002, **5**, 347.
18 A. Duthie, D. Dakternis, S. Daniele and L. G. Hubert-Pfalzgraf, manuscript in preparation.
19 K. G. Caulton and L. G. Hubert-Pfalzgraf, *Chem. Rev.*, 1989, **89**, 963.
20 J. A. Meese-Marktscheffel, R. Fukuchi, M. Kido, G. Tachibana, C. M. Jensen and J. W. Gilge, *Chem. Mater.*, 1993, **5**, 755; J. A. MM, R. Fukuchi, M. Kido, G. Tachibana, C. M. Jensen and J. W. Gilge, *Chem. Mater.*, 1993, **5**, 755; J. A. Meese-Marktscheffel, R. E. Cramer and J. W. Gilge, *Polyhedron*, 1994, **13**, 1045.
21 U. Bemm, R. Lashgari, R. Norrestam, M. Nygren and G. Westin, *J. Solid State Chem.*, 1993, **103**, 366.
22 S. C. Goel, M. Y. Chiang, P. C. Gibbons and W. E. Buhro, *Mater. Res. Soc. Symp. Proc*, 1992, **271**, 3.
23 A. R. Thani, M. Passacantando and S. Santucci, *Mater. Chem. Phys.*, 2001, **68**, 66.